$$Q_{q\alpha\beta}=\mathsf{S}\langle i\,|\,[\boldsymbol{\sigma}(1)-\boldsymbol{\sigma}(2)]_q\,|\,f\rangle\langle f\,|\,\sigma_\alpha(1)\sigma_\beta(2)\,|\,i\rangle, \quad \text{(A2)}$$

$$P_{qm}=\mathsf{S}\langle i\,|\,[\boldsymbol{\sigma}(1)-\boldsymbol{\sigma}(2)]_q\,|\,f\rangle\langle f\,|\,[\boldsymbol{\sigma}(1)+\boldsymbol{\sigma}(2)]_m\,|\,i\rangle. \quad \text{(A3)}$$

The symbols in Eqs. (A1)–(A3) have the following meanings: $|\,i\rangle$ is the initial triplet state; $|\,f\rangle$ is the final singlet state; S means average over the initial spin states and sum over the final spin states.

In order to apply the standard trace procedure, we have only to remember that we are working in the four-dimensional representation of two spin-$\frac{1}{2}$ particles (the three states of the triplet and the one of the singlet) and to introduce the projectors P_3 for the triplet and P_1 for the singlet, defined by

$$P_3=\tfrac{1}{4}[\boldsymbol{\sigma}(1)\cdot\boldsymbol{\sigma}(2)+3], \quad \text{(A4)}$$

$$P_1=\tfrac{1}{4}[1-\boldsymbol{\sigma}(1)\cdot\boldsymbol{\sigma}(2)]. \quad \text{(A5)}$$

Then we can rewrite Eqs. (A1), (A2), and (A3) in the following way:

$$Q_{qm}=\tfrac{1}{3}\,\mathrm{Tr}\{[\boldsymbol{\sigma}(1)-\boldsymbol{\sigma}(2)]_q\cdot\tfrac{1}{4}[1-\boldsymbol{\sigma}(1)\cdot\boldsymbol{\sigma}(2)] \times[\boldsymbol{\sigma}(1)-\boldsymbol{\sigma}(2)]_m\cdot\tfrac{1}{4}[3+\boldsymbol{\sigma}(1)\cdot\boldsymbol{\sigma}(2)]\}, \quad \text{(A6)}$$

$$Q_{q\alpha\beta}=\tfrac{1}{3}\,\mathrm{Tr}\{[\boldsymbol{\sigma}(1)-\boldsymbol{\sigma}(2)]_q\tfrac{1}{4}[1-\boldsymbol{\sigma}(1)\cdot\boldsymbol{\sigma}(2)] \times[\sigma_\alpha(1)\sigma_\beta(2)]\cdot\tfrac{1}{4}[3+\boldsymbol{\sigma}(1)\cdot\boldsymbol{\sigma}(2)]\}, \quad \text{(A7)}$$

$$P_{qm}=\tfrac{1}{3}\,\mathrm{Tr}\{[\boldsymbol{\sigma}(1)-\boldsymbol{\sigma}(2)]_q\cdot\tfrac{1}{4}[1-\boldsymbol{\sigma}(1)\cdot\boldsymbol{\sigma}(2)] \times[\boldsymbol{\sigma}(1)+\boldsymbol{\sigma}(2)]_m\cdot\tfrac{1}{4}[3+\boldsymbol{\sigma}(1)\cdot\boldsymbol{\sigma}(2)]\}. \quad \text{(A8)}$$

The evaluation of the traces in these equations is now obvious and the results are

$$Q_{qm}=\tfrac{2}{3}\delta_{qm}, \quad \text{(A9)}$$

$$Q_{q\alpha\beta}=\tfrac{2}{3}i\epsilon_{q\alpha\beta}, \quad \text{(A10)}$$

$$P_{qm}=0. \quad \text{(A11)}$$

PHYSICAL REVIEW C VOLUME 1, NUMBER 3 MARCH 1970

Extension of the Optical Model and Its Application to the Elastic Scattering of ^{16}O by ^{16}O Nuclei*

R. A. Chatwin, J. S. Eck,† and D. Robson‡
Department of Physics, Florida State University, Tallahassee, Florida 32306
and
A. Richter§
Department of Physics, Florida State University, Tallahassee, Florida 32306 and Argonne National Laboratory, Argonne, Illinois 60439

(Received 28 May 1969; revised manuscript received 6 November 1969)

The absorptive part of the optical potential is considered as a function of conserved quantum numbers such as the total angular momentum J. This investigation results in the introduction of a smooth cutoff in the strength of the absorptive potential as J gets larger than a certain critical value. This value is typical of nonelastic channels, and the cutoff reflects poor matching between the angular momenta in the elastic channel and those in the nonelastic channels. Brief consideration is also given to other conserved or approximately conserved quantum numbers such as isobaric spin and parity. The standard optical potential is modified to include an angular-momentum dependence with a suitable cutoff, and is applied to the elastic scattering of ^{16}O by ^{16}O nuclei. In the energy range 15–36 MeV(c.m.), such an extended optical model gives a good description of all the gross features of the ^{16}O-^{16}O data. A repulsive core in the ^{16}O-^{16}O potential has been considered, but no definite evidence for it is found in the present analysis.

I. INTRODUCTION

In this paper, we demonstrate the dependence of the imaginary part of the optical model on conserved quantum numbers and modify the optical model qualitatively by introducing a cutoff in the strength of the absorption potential for high angular momentum. Some applications of this simple model, embodying the principle of matching angular momentum and energy in the entrance and exit channels, have already been published.[1,2] Here, we present an application to the elastic scattering of nuclei (namely, ^{16}O by ^{16}O) at energies above the Coulomb barrier.[3]

In Sec. II, the modification of the optical model is

* Work supported in part by the U.S. Air Force Office of Scientific Research, Office of Aerospace Research, United States Air Force, under AFOSR Grant No. AF-AFOSR-69-1674, the National Science Foundation Grants Nos. GP-7901 and NSF-GP-5114, and the U.S. Atomic Energy Commission.

† Present address: Kansas State University, Manhattan, Kans. 66502.

‡ Alfred P. Sloan Research Fellow.

§ On leave of absence from the Max-Planck-Institut für Kernphysik, Heidelberg, Germany. Present address: Argonne National Laboratory, Argonne, Ill. 60439.

[1] A. Bisson and R. H. Davis, Phys. Rev. Letters **22**, 542 (1969).

[2] R. A. Chatwin, J. S. Eck, A. Richter, and D. Robson, in *Nuclear Reactions Induced by Heavy Ions* (North-Holland Publishing Co., Amsterdam, to be published); J. S. Eck, R. A. Chatwin, K. A. Eberhard, R. A. LaSalle, A. Richter, and D. Robson, *ibid.*

[3] R. H. Siemssen, J. V. Maher, A. Weidinger, and D. A. Bromley, Phys. Rev. Letters **19**, 369 (1967).

justified from a definition of the optical operator[4] in terms of projection operators. For heavy ions, the simple meaning of the modification is that the heavy masses in the entrance channel may carry in a greater angular momentum than can be carried away in any exit channel (which typically would have no particle heavier than an α particle). If the conserved quantum number of the resonance can find no matching probability in any exit channel, single-particle resonances may occur where they have hitherto been unexpected.

In Sec. III, we shall show how this model is able to describe the major features of the ^{16}O-^{16}O elastic scattering from 15 to 36 MeV (c.m.).[3] However, it is useful to discuss first the relative success of other attempts[3,5–7] to describe the ^{16}O-^{16}O data. In Sec. III, we also give a brief report of an unsuccessful attempt to find evidence for a repulsive core in the ^{16}O-^{16}O interaction. The extended version of the optical model is able to reproduce all the significant features of the gross structure, and comparisons between such modified calculations and calculations with a standard optical model show that (i) the excitation functions at angles less than 90° are indeed[3] predominantly due to diffraction, i.e., they correspond to the movement of a diffraction pattern with changing energy (wavelength), but (ii) close to 90° the structures are broad resonances of single partial waves. These resonances of large J do not suffer great absorption because of the matching condition described in Sec. II.

In Sec. IV, we present a fit to the ^{16}O-^{16}O excitation functions by use of our extension of the optical model.

Section V is a summary of the results, together with some further remarks about the repulsive core and the resonances. In the Appendix, a classical model of the L-cutoff parameter is presented.

II. A NECESSARY EXTENSION OF THE OPTICAL MODEL

The standard optical model of nuclear physics uses the imaginary potential $W(r)$ to describe the absorption of the incoming waves into reaction and inelastic outgoing channels. As the incoming energy E is increased, more such channels become available to the system. The probability for absorption per unit volume, which is proportional to W, must increase, on the average, as the available energy increases. To represent this behavior, $W(r)$ is made a growing function of E.

However, one important effect of nuclear physics is not explicitly considered in this form of the optical model: Angular momentum and energy must be simultaneously conserved in the reaction channels. For a given energy E, there exists in each channel a maximum angular momentum J_c' beyond which the absorption potential is negligible, whereas at present the optical model implies that the absorption per unit volume is the same for all incoming waves.

This possibility appears to be most conveniently discussed by use of the optical operators of the Feshbach formalism.[4] Define P_c to be the projection operator that gives elastic scattering in channel c and $Q_c=1-P_c$ to be the projector onto nonelastic channels. Then the optical operator in channel c is[4]

$$H_c^{\rm opt}(E)=P_cHP_c\sum_n\frac{P_cHQ_c\,|\,n\rangle\langle n\,|\,Q_cHP_c}{E_n-E}+\frac{\mathcal{P}}{\pi}\int_{E_a'}^{\infty}\frac{W_c^{\rm opt}(E')\,dE'}{E'-E}+iW_c^{\rm opt}(E),\quad(1)$$

in which the absorption operator is

$$W_c^{\rm opt}(E)=-\pi\sum_\nu P_cHQ_c\,|\,\nu,E\rangle\langle\nu,E\,|\,Q_cHP_c,\qquad E>E_a'$$
$$=0,\qquad E\leq E_a'.\quad(2)$$

The states $|\,n\rangle$ and $|\,\nu,E'\rangle$ are bound and continuum eigenstates of the operator Q_cHQ_c with eigenvalues E_n and E', respectively. The sum over ν allows for several states with the same energy, and the lower limit of the principal-value integration E_a' is the threshold energy for the most energetically open channel a'. The operator $H^{\rm opt}$ is diagonal in total angular momentum and parity, and the absorptive part of $H^{\rm opt}$ conserves energy in the intermediate states $|\,\nu,E\rangle$. Since P_cHQ_c conserves angular momentum and parity, the elastic scattering channel with a given value of J^π couples only to states $|\,n\rangle$, $|\,\nu,E'\rangle$ with the same value of J^π so that, in general, $H_c^{\rm opt}$ is J^π-dependent.

In the absorptive part of $H_c^{\rm opt}$, we notice that the intermediate states simultaneously conserve J^π and E, whereas this is not true for the Hermitian part of $H_c^{\rm opt}$ since the intermediate states are off the energy shell. We do not make quantitative arguments about the J^π dependence of Eqs. (1) and (2), but we can deduce certain qualitative features.

The states $|\,\nu,E\rangle$, by construction, do not involve any incident-channel contributions, and the degree of overlap with the rotationally invariant operators P_cHQ_c and Q_cHP_c is therefore viewed as a function of the *nonelastic* angular momentum

$$\mathbf{J}'=\mathbf{L}'+\mathbf{I}_1'+\mathbf{I}_2'\quad(3)$$

that can be carried away in the various final states[8]—provided that for the moment we restrict our discussion

[4] H. Feshbach, Ann. Phys. (N.Y.) **5**, 357 (1958); **19**, 287 (1962).
[5] B. Block and F. B. Malik, Phys. Rev. Letters **19**, 239 (1967).
[6] W. Scheid, R. Ligensa, and W. Greiner, Phys. Rev. Letters **21**, 1479 (1968).
[7] R. J. Munn, B. Block, and F. B. Malik, Phys. Rev. Letters **21**, 159 (1968).

[8] Primed angular momenta are associated with an exit channel; unprimed variables go with the entrance channel. Thus, we have denoted the cutoff parameter by J_c', which may help avoid confusion with the cutoff in strong-absorption models.

to the case of two-body breakup.[9] As J gets larger, the states $|\nu, E, J^\pi\rangle$ have a smaller overlap with the short-ranged operator P_cHQ_c (Coulomb excitation is ignored) as a result of the increasing repulsion of the combined angular momentum and Coulomb barriers associated with the increasing angular momentum L'. Consequently, the strength of the optical operator corresponding to absorption should decrease as J exceeds a certain value J_c', which is characteristic of the *nonelastic* channels. The same argument cannot be applied to the Hermitian part of $H^{\rm opt}$ because the intermediate states do not have a definite energy. The arguments above are not much affected by our restriction to two-body channels. Multiproduct channels can be discussed in a similar manner if L' in Eq. (3) is interpreted as the sum of all the orbital angular momenta of relative motion and $I_1'+I_2'$ is replaced by the sum of all of the products.

The above arguments are also only qualitative because we have not used the energy-averaged operator corresponding to shape-elastic scattering. The conventional theoretical procedure for performing an energy average is to replace E by the complex energy $E+iF_c$. The result is the shape-elastic operator

$$\bar{H}_c^{\rm opt}(E)=P_cHP_c-P_cHQ_c \times(Q_cHQ_c-E-iF_c)^{-1}Q_cHP_c-iF_c, \quad (4)$$

with an absorption operator given by

$$\bar{W}_c^{\rm opt}(E)=-F_c\left(1+\sum_n \frac{P_cHQ_c\,|\,n\rangle\langle n\,|\,Q_cHP_c}{(E_n-E)^2+F_c^2} + \sum_\nu \int_{E'}^\infty dE' \frac{P_cHQ_c\,|\,\nu, E'\rangle\langle\nu, E'\,|\,Q_cHP_c}{(E'-E)^2+F_c^2}\right). \quad (5)$$

Now, in Eq. (5), energy is not conserved exactly in the intermediate states, but it is conserved with an error of order $\pm F_c$. Of course, as a simple calculation shows, the unaveraged operator Eq. (2) is connected to Eq. (5) through the relation

$$W_c^{\rm opt}(E)=\lim_{F_c\to 0^+}\bar{W}_c^{\rm opt}(E), \quad (6)$$

so that the arguments used above for the operator $W_c^{\rm opt}(E)$ will apply accurately to $\bar{W}_c^{\rm opt}(E)$ only when $F_c\ll E$.

In order to consider the situation in which F_c is not sufficiently small, it is important to consider the reason for introducing the quantity F_c. Its role is to smooth out any rapid variation of $H_c^{\rm opt}(E)$ with energy, which may occur in nuclear physics because of the many-body (compound-nucleus) components of the intermediate states. The smallest energy interval $F_c(E)$ that one may choose should be related to the coherence width, the amplitude, and the density of the many-body (compound-nucleus) components in $|\nu, E\rangle$ or $|n\rangle$; yet ideally it should not be chosen so large that the one-body potential resonances are completely smoothed out. Conventionally, $F_c(E)$ is assumed to be independent of the total angular momentum, so that the optical-model calculations can be compared with the energy-averaged cross sections via the relation

$$\langle\sigma\rangle=\sigma^{\rm opt}+\sigma^{\rm ce}, \quad (7)$$

where $\sigma^{\rm ce}$ is the compound-elastic contribution and $\sigma^{\rm opt}$ is the optical-model simulation of the shape-elastic cross section.

In most situations of interest, many exit channels are energetically allowed, so that if one ignores angular-momentum mismatching (as in the conventional optical model), it appears reasonable to ignore $\sigma^{\rm ce}$ effects. However, in the extended version of the optical model, the number of exit channels that compete with the entrance channel may decrease strongly as J increases beyond J_c'. In this event, it is not clear that $\sigma^{\rm ce}$ can be ignored. On the other hand, it is unlikely that $\sigma^{\rm ce}$ can be usefully calculated in such situations for two reasons: (i) The statistical assumptions usually used to calculate compound-nucleus cross sections are expected to be invalid for $J>J_c'$, because the level density of compound states becomes too small for large J values, and (ii) even if statistical methods are valid, the rapid change in the number of competing exit channels in the transition region around $J\approx J_c'$ makes a Hauser-Feshbach type of calculation intractable.

The important result of the above considerations is that shape-elastic scattering should be calculated by use of an absorption operator that satisfies

$$\bar{W}_c^{\rm opt}(E)\to F_c, \qquad J>J_c' \quad (8)$$

where F_c is the minimum energy interval that suffices to smooth out the many-body features in all partial waves.

We now investigate the importance of Eq. (8). If the absorption is removed and one calculates the real phase shifts for the real part of the potential, there is an upper value $J=J_0$ beyond which the nuclear phase shift is negligible.[10] There are then two situations of interest: (a) $J_c'\geq J_0$ and (b) $J_c'<J_0$.

Case (a) is typical of most nucleon scattering because these channels carry little orbital angular momentum compared to channels with more massive products. In these circumstances, the inclusion of a cutoff in $W_c^{\rm opt}$ for partial waves with $J>J_c'>J_0$ has no effect because they already have no phase shift and therefore cannot be absorbed.

Case (b) occurs in the elastic scattering of some heavy ions, in those regions of energy in which the predominant exit channels involve smaller masses than

[9] For two-body channels, the spins I_1', I_2' of the products are not very large in physical systems, so that J' in these channels is large only when L' becomes large.

[10] The existence of a phase shift is not a necessary condition for absorption. However, in the use of the optical model in nuclear physics, the imaginary potential has roughly the same radial extension as the nuclear potential. Therefore, a partial wave begins to be absorbed at the same energy at which it begins to feel the nuclear potential.

the entrance channel; if the Q value of the channel is not too large, smaller masses imply smaller characteristic values of the orbital angular momenta. For such projectiles as ^{16}O there are three major types of exit channels: those with equal or similar mass (e.g., inelastic scattering), those with a smaller mass (e.g., α particle), and those with many product particles. The first type of channel leads to $J_c'<J_0$ if the Q value is negative and not negligible and intrinsic spins not too large. If this condition holds at all, it will normally hold at low energies since the variation of J with energy is less rapid in the entrance channel than in the exit channel. The moment of inertia is less in the second type of channel, and hence J_c' increases less rapidly with energy than does J_0. Even if at low energies $J_c'>J_0$, so that the poor matching is unimportant, there will exist a higher energy above which $J_c'<J_0$. Finally, there will be a threshold above which the system breaks up into many particles (as possibly neutron evaporation, which has large total J') and $J_c'>J_0$ for this energy and all higher energies.

Let us summarize these principles. There is always a J cutoff in the absorptive term $W(r)$. This cutoff would not be expected to be effective in some experiments such as nucleon-nucleus scattering. In the general system of two heavy ions, there will be three energy regions: (i) At the lowest energies (with $J_c'>J_0$), the standard form of the optical model is valid, (ii) in an intermediate region (where $J_c'<J_0$), the standard model is invalid, and the cutoff ought to be included, and (iii) at high energies (where again $J_c'>J_0$), the standard model is again valid. In a particular system, either of the first two regions may have shrunk and disappeared.

The simplest model containing a smooth J cutoff in absorption is

$$W^J(r)=W(r)\{1+\exp[(J-J_c')/\Delta J']\}^{-1}, \quad (9)$$

where J_c' is an average characteristic cutoff in angular momentum for the nonelastic channels, and $\Delta J'$ reflects the physical uncertainty arising from uncertainty in L_c' and from the various possible spin values I_1', I_2' which blur the relation between J_c' and L_c'. If energy averaging is important, then the first term in Eq. (5) must be taken into account by adding $\sim F_a$ to the right-hand side of Eq. (9). In this way, condition (8) is properly satisfied.

In general, the cutoff J_c' is a function of energy because the maximum angular momentum increases as energy increases. The simplest prescription, in view of the above discussion, appears to be

$$J_c'=k_c'(E)R_c', \quad (10)$$

where $k_c'(E)$ represents an average wave number for the nonelastic channels and R_c' reflects the average size of the Q_cHQ_c system. [A classical derivation of Eq. (10) is given in the Appendix.]

When inelastic channels are important, there are two obvious prescriptions, each having a minimal set of parameters. Either one can use Eqs. (9) and (10), or one can deal with the inelastic channels by a coupled-channel calculation. In the latter, one needs an absorption matrix having a cutoff J_c' typical of reaction channels other than inelastic channels. This is currently being investigated, and the results will be reported later. In the present article, σ^{oe} is ignored, and the model of Eq. (9) is used to investigate ^{16}O-^{16}O scattering. Other calculations using Eq. (9), or some simple variant of it, have been reported already[1,2]; they give considerable support to this simple model. The absorption potential is simply an L-dependent one in the case of scattering of a spin-zero projectile by a spin-zero target, so that Eq. (9) becomes

$$W^L(r)=W(r)\{1+\exp[(L-J_c')/\Delta J']\}^{-1}. \quad (11)$$

We conclude this section by noting that the absorption potential will, in general, depend on *each* conserved (or approximately conserved) quantum number whenever the overlap between intermediate states $|\nu, E\rangle$ and the coupling operators P_cHQ_c, Q_cHP_c is a strong function of these quantum numbers.

The most striking prediction is the possible occurrence of relatively pure single-particle (or single-cluster) resonances with particular quantum numbers J, π, or T. For *total angular momentum*, such resonances will require large values of $J(>J_c')$ and a real potential $\tilde{V}_c^{\text{opt}}$ that is able to support them. Such a situation is now believed to have been observed in ^{16}O-^{40}Ca scattering.[2] For *isospin*, the phenomenon is well known from the recent work on analog resonances in which the $T_>$ absorption strength is shown to be very small relative to the $T_<$ absorption strength. This difference mirrors the difference in the number of isospin-allowed decay channels, and the compound-nucleus character of the two types of states; i.e., the level density of $T_<$ states is often a million or more times that of the $T_>$ states. The same type of situation may also exist for *parity*, because in many nuclei the level density of states of each parity (and perhaps a certain J) is quite different; e.g., the first negative-parity state in even-even nuclei may be as high as 10-MeV excitation. This possibility is yet to be investigated.[11]

III. DIFFRACTION AND ORBITING

In the elastic scattering of ^{16}O ions by ^{16}O, there is a striking contrast between the excitation functions near the Coulomb barrier and those at higher energies. The height of the Coulomb barrier is about 11 MeV. The experimental cross sections[12] are featureless near this energy, except for the break from pure Coulomb

[11] A yet more general approach would consider projections onto other subspaces—this being necessary to describe situations different from those described explicitly here (e.g., the dipole states in photonuclear reactions).

[12] D. A. Bromley, J. A. Kuehner, and E. Almquist, Phys. Rev. **123**, 878 (1969).

scattering. Above a c.m. energy of 16 MeV, gross structure appears[3] with broad and deep oscillations as well as finer structure (Fig. 1).

There have been several explanations of the gross structure in these data. In this section, we shall describe how the relative successes of each hypothesis leads one to use the extension of the optical model described in Sec. II.

In a previous paper,[13] we showed that the conventional optical model is an adequate description of the experiments near the Coulomb barrier. Of particular interest in that work was the possible repulsive core[3,5,6,14] in the interaction of the two nuclei. The effect of any core is masked by the Coulomb barrier, by the centrifugal barrier, and by the attenuation of the wave function inside the nucleus because of absorption into nonelastic channels.

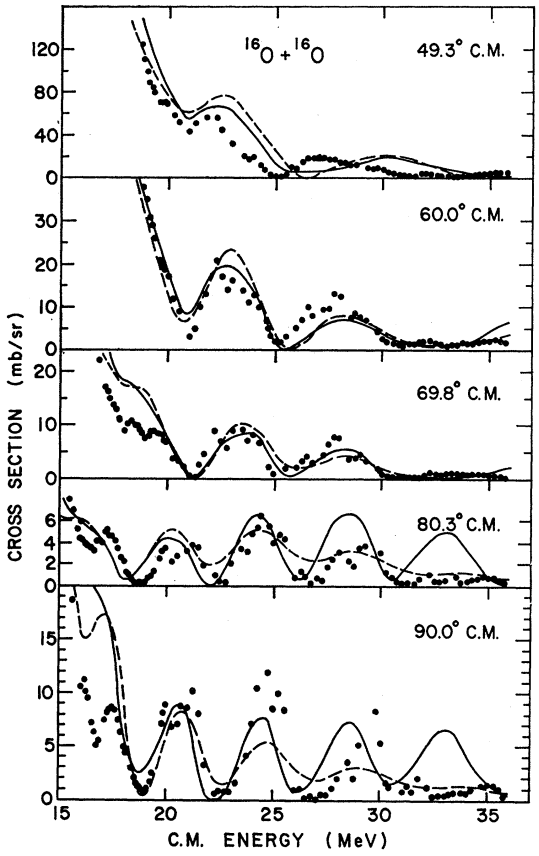

FIG. 1. Excitation functions for ^{16}O-^{16}O elastic scattering. The data points from Ref. 3 have an absolute error of ±15%. The calculated curves show the relative abilities of the standard optical model and of its extension in describing the data. They are not parameter fits. The dashed curve is for the standard optical model with $U=17$ MeV, $R=6.8$ F, $a=0.49$ F, and $W=0.1E$. The full curve is for the L-dependent absorption, with $W=0.22E$, $\bar{Q}=-6.7$ MeV, $\bar{R}=6.7$ F, and $\Delta J'=0.4$. The calculations include no contribution from the compound nucleus.

Does the structure of the higher-energy data contain evidence for a repulsive core? In the excitation functions, the peculiarities of gross structure that must be considered are (a) the regular spacing of the peaks and valleys, (b) the large peak-to-valley ratios, (c) the flatness of the valleys at 90° (c.m.), and (*d*) the shift in the angular positions of the peaks and valleys.

Two recent papers[6,7] have proposed using a molecular type of potential for the higher-energy data. With an imaginary potential based on qualitative arguments, the calculations in Ref. 6 corresponded fairly well to the experimental oscillations. An example of a real molecular potential was considered in Ref. 7. Absorption was taken into account by cutting off the effect of all partial waves for which $L\leq 12$. The 90° excitation function for this model has a broad oscillation with a large peak-to-valley ratio, and also some fine-structure peaks.

What happens to the calculated scattering when a repulsive core is not used? Nothing essential changes. For example, the optical model, with purely attractive potentials, is known[3] to give oscillations in the excitation functions. The model of Ref. 6 has similarly an absorptive term and a potential barrier, and the two calculations are much alike. A calculation as in Ref. 7, but with the core removed, also shows similar structure.[15] The mere production of such structure from a calculation with a core is not sufficient evidence for a core. The interaction in the interior of the nucleus is masked by potential barriers and by absorption.

Our thesis is that the gross oscillations are of two classes: (i) diffraction patterns in a cone of small angles ($\theta<80°$, say, in the energy range of Fig. 1) and (ii) a cone of larger angles ($\theta\lesssim 90°$) dominated by broad orbiting[16] resonances. For example, we have calculated phase shifts and excitation functions, at angles less than 90°, with the model of Ref. 7. The broad resonance in the 90° calculation is produced by a phase shift that rises at an energy near the top of the effective potential, i.e., at the maximum of

$$V_L(r)=V_{\text{nuc}}(r)+\hbar^2L(L+1)/2\mu r^2+V_c(r), \quad (12)$$

where

$$\begin{aligned} V_c(r)&=Z^2e^2/r, && r\geq c\\ &=Z^2e^2(3c^2-r^2)/2c^2, && r<c \end{aligned} \quad (13)$$

is the Coulomb potential and μ is the reduced mass. The interference effects that were reported in Ref. 7 are

[13] R. A. Chatwin, J. S. Eck, A. Richter, and D. Robson, Phys. Rev. **180**, 1049 (1969).

[14] K. A. Brueckner, J. R. Buchler, and M. M. Kelly, Phys. Rev. **173**, 944 (1968).

[15] The cores used in Ref. 7 are of longer range than the attractive potential, so that removing the core decreases the barrier height, and shifts the structures in the calculation to lower energies.

[16] K. W. Ford, D. L. Hill, M. Wakano, and J. A. Wheeler, Ann. Phys. (N.Y.) **7**, 239 (1959). By "orbiting resonance" we shall mean the single-cluster resonance that occurs near the top of an effective-potential barrier. Other resonances below this energy we shall classify arbitrarily as "sharp resonances" because they tend to have smaller natural widths.

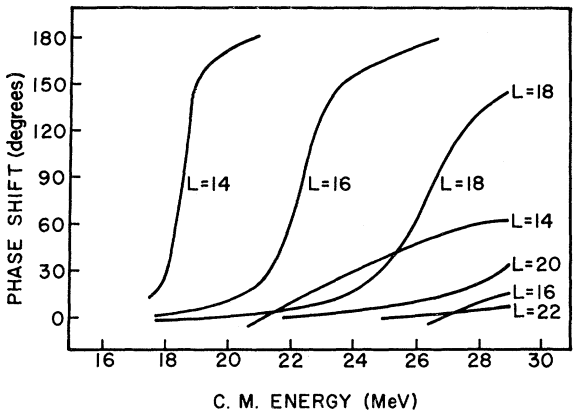

FIG. 2. Phase shifts for $L \geq 14$ calculated for the real potential of Fig. 1.

isolated sharp resonances of higher partial waves which are below their orbiting energy: A sharp spike is superposed on the smooth orbiting cross section.

In this model, increasing the energy does not result in absorption of partial waves higher than $L=12$. Therefore, we found that the peaks in the excitation functions at other angles always occur at energies identical to those of the resonances. We shall next describe the heuristic value of these calculations after first taking a look at the type of calculation reported by the original experimenters.[3]

Davis and Aldridge[17] pointed out that the ^{16}O-^{16}O elastic scattering structures could be described as the successive absorption of partial waves with changing energy. They discussed only the 90° excitation function and needed to hypothesize a resonating phase shift for each peak. We have a hint that such resonances might come from an orbiting phenomenon.

The optical model includes diffraction and orbiting in a general way. If the absorptive term $W(r)$ is infinite for all radii $r \leq r_0$, say, the resulting scattering will be pure diffraction of waves on a black ball of radius r_0. If $W(r)$ is finite, there is also a probability for transmission and reflection in the real potential. This is the physical significance of the optical-model description of the data in Ref. 3. They used the standard Woods-Saxon optical potential with parameter set 1, namely, $U=17$ MeV, $R=6.8$ F, $a=0.49$ F, and a volume absorption $W(r)$ of the same radius. Such a shallow potential was suggested by Block and Malik[5] and has been shown[13] to be consistent with the elastic scattering data from 10 to 14 MeV (c.m.). Using $W=0.1E_{\text{c.m.}}$ (chosen because $W=1.3$ MeV gave an excellent fit[13] to the 13-MeV angular distribution) leads to a good description of the gross structure in the excitation functions (Fig. 1) in the range 15–36 MeV (c.m.). The valleys in the cross sections are too shallow, but the angular dependence is reproduced. We have set the Coulomb parameter $c=5.0$ F, which is twice the rms radius of proton centers for ^{16}O nuclei. (Small changes in this Coulomb parameter do not affect the optical-model calculations.) As an estimate, absorption begins for that partial wave which reaches the top of the effective barrier in $V_L(r)$. The maxima occur at some radius r_m just outside the Woods-Saxon half-strength radius R, say at

$$r_m \approx R+2a. \tag{14}$$

Now, $V_L(r)$ has a maximum value of 21.7 MeV for $L=16$, so the separation between the absorption of that partial wave and that due to the next one ($L=18$) is given by

$$\Delta_D \approx V_{L+2}(r_m) - V_L(r_m) = \hbar^2(2L+3)/\mu r_m^2, \tag{15}$$

which gives a diffraction-peak spacing $\Delta_D \approx 3$ MeV. This compares well with the calculations in the optical model (Fig. 1), and supports the physical interpretation given above.

Figure 2 shows some of the phase shifts for (real) potential set 1. There are no resonances other than for orbiting, because the potential well is too shallow to support any. The orbiting amplitudes give rise to the oscillations at 90°, in competition with the absorption effects described above. The spacing of these resonances is given by

$$\Delta_R \approx V_{L+2}(r_m) - V_L(r_m) = \Delta_D. \tag{16}$$

Absorption takes place soon after a partial wave begins to resonate.

As expected from Ref. 3, we find that a description of ^{16}O-^{16}O elastic scattering by the standard optical model can successfully represent the broad peaks at various angles. However, the valleys at 90° cannot be made low enough relative to the peaks, because the absorption of the orbiting partial waves averages out the resonances, thus filling up the valleys.

Then, the two types of calculation, the one of Ref. 7 and the other of Ref. 3 (a standard optical model), give complementary results. The former (using real amplitudes) gives large peak-to-valley ratios at 90°; the latter gives the correct variation of the major structures with changing angle. The experimental data, therefore, require that there be (i) normal absorption of the low partial waves, which dominate the lower-angle diffraction patterns, and (ii) little absorption of the orbiting partial waves, which dominate the resonances at 90°. The principle of angular-momentum matching that we have included in an extended version of the optical model (Sec. II) is suitable for this situation.

Let us approximate Eq. (11) by

$$J_c' = L_c' = (2\mu/\hbar^2)^{1/2}\bar{R}(E+\bar{Q})^{1/2}, \tag{17}$$

where $\bar{R}$ and $-\bar{Q}$ represent some average values of the radius and the effective threshold for the predominant nonelastic channels. The choice $\bar{R}=6.7$ F and $\bar{Q}=-6.7$ MeV yields $J_c'=16$ at 21.8 MeV and $J_c'=18$ at 25.8 MeV. Then, part of the $L=16$ and $L=18$ resonances (Fig. 2) will contribute to the two broad peaks

[17] J. P. Aldridge and R. H. Davis, discussed by R. H. Davis, J. Phys. Soc. Japan Suppl. 24, 264 (1968).

at 20.5 and 24.5 MeV in the 90° excitation function. Other particular values of J_c' obtained with Eq. (17) are $J_c'=14$ at 18.3 MeV, $J_c'=20$ at 30.3 MeV, and $J_c'=22$ at 35.3 MeV. Physically, one would expect several channels to successively open and become important in Eq. (10) as the energy varies over the range 15–36 MeV (as discussed in Sec. II). Thus, the single choice of $\bar{R}$ and $\bar{Q}$ will not be realistic throughout this energy range. In particular, we have not yet attempted to fit the data; instead, we leave the real potential of Ref. 3 unchanged (set 1) and vary the absorption W in direct proportion to the c.m. energy E to correct the magnitude of the cross sections.

The parameter $\Delta J'$ was chosen to be 0.4. Calculations showed that the cross sections were not sensitive to variations in this value. For α-^{28}Si scattering, the transmission coefficients rise quite rapidly with E in the range from $L=16$ to 18, and since such a channel is likely to be dominant at $L\approx16$–18, this value of $\Delta J'$ is easily justified.[2]

The calculated and experimental excitation functions are shown in Fig. 1. The two calculations, with and without the L dependence, of the cross sections at 49.3°, 60.0°, and 69.8° c.m. differ little, i.e., the extended optical model has retained the description of the diffraction structures. This can be better seen in a comparison of angular distributions calculated in the two models (Fig. 3). Up to about 75°, the diffraction patterns are similar, and any difference is not obviously significant. But from 75° to 90° and in a minimum of

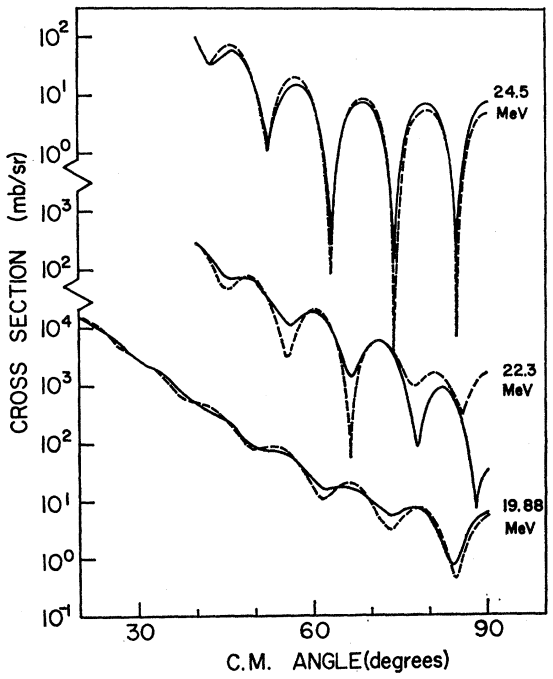

FIG. 3. Three angular distributions for the ^{16}O-^{16}O elastic scattering. The calculated curves are for the standard optical model (dashed line) and for the optical model with an L-dependent absorption (solid line), as in Fig. 1.

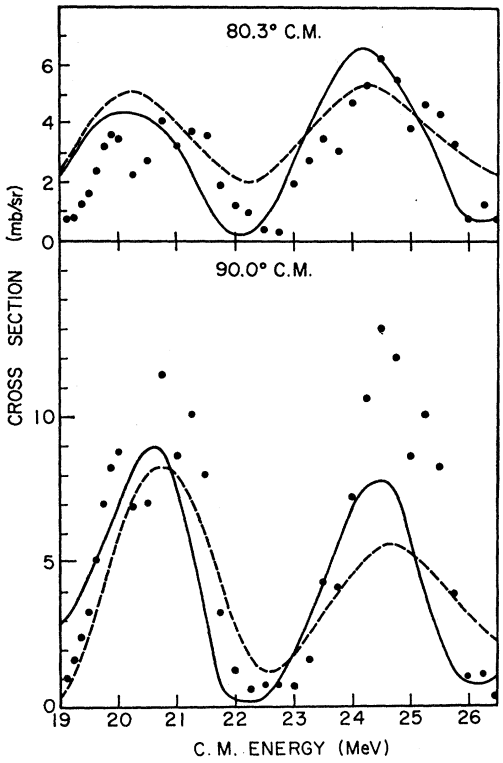

FIG. 4. Detail of the calculated and experimental excitation functions in Fig. 1.

the 90° excitation function (22.3 MeV), the conventional optical model and the extended version that we propose do not give the same results. Figure 4 is a magnified picture of part of the cross sections at 80.3° and 90° c.m. At these angles, the extended optical model gives a much better description of the main features of the data than does the standard model. In particular, the peak-to-valley ratios are large, and the valleys at 90° are flat. This completes what we set out to show: The information carried in the gross structures of the ^{16}O-^{16}O elastic scattering can be described with an angular-momentum cutoff in $W(r)$.

In Fig. 4, the calculated structures are slightly out of phase with the data. This appears to be a sensitive test of the height of the barrier for these high L values. If the real potential were changed to make the barrier slightly higher, the orbiting resonances (which cause the rise in the 90° cross sections) would occur at higher energies.

IV. DESCRIPTION OF THE ^{16}O-^{16}O ELASTIC SCATTERING

Now that we have seen what the new calculations have changed and what is left unchanged from the standard optical model, we have attempted to fit (by eye) all the excitation functions from 15 to 36 MeV. First, the real potential U was changed to position the resonances at 90°. The new parameters are $U=16$ MeV, $R=6.8$ F, $a=0.49$ F. The imaginary potential was left

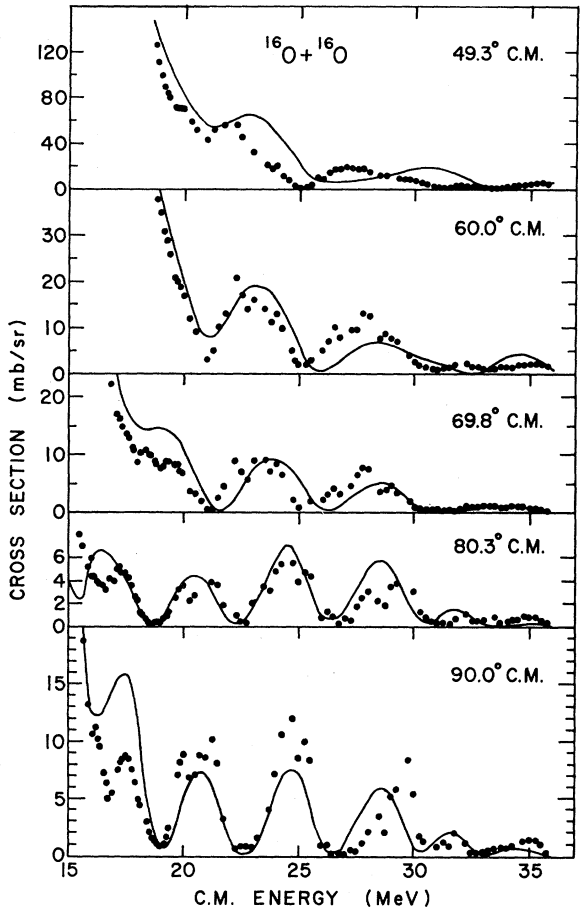

FIG. 5. Fit to the excitation functions of Ref. 3 using angular-momentum matching in the optical model. Parameters for the calculation are given in the text, Sec. IV.

with unchanged radial dependence, but with a new energy dependence $W=0.5E_{\text{c.m.}}-7$. The relatively minor parameter $\Delta J'=0.4$ was not altered. Figure 5 shows a fit to the data, with J_c' a continuous and increasing function of E defined by Eq. (17), and

$$\bar{R}=5.4\text{ F}, \quad \bar{Q}=1.7\text{ MeV} \quad \text{for } 15.<E_{\text{c.m.}}<23.8\text{ MeV},$$
$$\bar{R}=6.9\text{ F}, \quad \bar{Q}=-8.1\text{ MeV} \quad \text{for } 23.8<E_{\text{c.m.}}<29.7\text{ MeV},$$
$$\bar{R}=9.0\text{ F}, \quad \bar{Q}=-17\text{ MeV} \quad \text{for } 29.7<E_{\text{c.m.}}<36.\text{ MeV}.$$

The calculation is quite faithful to the observed structure over the whole energy range.[18]

[18] The diffraction peaks at 49.3° have the correct structure both in the present calculation and in the regular optical model (Ref. 3). However, both calculations are out of phase with the data; changing the real potential or the cutoff in $W(r)$ does not affect this detail. These are the two parts of the optical model that we wished to investigate in this work.

Splitting up the energy dependence of J_c' into the three domains is in accord with the remarks of Sec. II about the dominance of the three sorts of reaction channels. In particular, the average channel radius $\bar{R}$ and the average threshold $-\bar{Q}$ increase with energy. Also, the J dependence is most significant in and around the central domain; at the highest and lowest energies, there is no significant improvement over the standard optical model.

In our *calculations*, a single partial amplitude dominates the peaks at 21, 25, 29, 32, and 35 MeV with $J=16$, 18, 20, 22, and 24, respectively.

V. CONCLUSIONS

The results of this work on ^{16}O-^{16}O scattering well above the Coulomb barrier, and of theoretical studies[13] of the data near the Coulomb barrier, show that no obvious effects of "molecular" potentials can be seen in the gross structure of the excitation functions. For that reason, one should not use such potentials *a priori* in a phenomenological description of the data. An *a priori* choice of a molecular potential has been used recently[19] in a phenomenological description of the first small structure in the data, i.e., the oscillation at 15–17 MeV. It is interesting that the result is no worse when one uses no repulsive core but only the standard attractive potentials of the optical model (Fig. 1). The success of a shallow[3,5] interaction (only 17 MeV deep) in fitting the data at all these energies may point *indirectly* to the existence of a repulsive core.

The gross structure of the excitation functions at higher energies is fairly well described by the standard optical model[3] but neither the large peak-to-valley ratios of the data nor the broad valleys appear in the calculated cross sections until an L-dependent absorptive potential is introduced.

This L-dependent imaginary term is not an arbitrary extension of the optical model, but has a physical origin related to the angular momentum of the reaction channels. Moreover, it is expected to apply to all cases of nuclear scattering, though the effects of it should be most easily observed in heavy-ion scattering involving spherical nuclei.

Resonant phase shifts for $L=16$, 18, and 20 contribute large amplitudes to the elastic scattering in the energy ranges 19.5–22.0, 23.0–25.5, and 27.5–31.0 MeV, respectively. These regions are where orbiting occurs; the two nuclei spend a long time close together, and therefore enhance the probabilities of any reaction or inelastic process. This single-particle (or single-cluster) phenomenon might be called an orbiting giant resonance.

If $W(r)$ is a very strong absorptive potential, an orbiting resonance will be smeared out too much to be seen. Otherwise, the criterion for the appearance of such giant resonances is the coincidence of absorption and

[19] L. Rickertsen, B. Block, J. W. Clark, and F. B. Malik, Phys. Rev. Letters **22**, 951 (1969).

orbiting [expressed by Eq. (16)]. This is satisfied if the radii of the real and absorptive potentials are equal, as one would expect for nuclei that are not easily deformed. If the absorptive potential has a larger range than the real potential, then a partial wave will be absorbed before orbiting can occur.

ACKNOWLEDGMENTS

We thank Dr. J. V. Maher and Dr. R. H. Siemssen for making their experimental data available to us. One of us (A.R.) also gratefully acknowledges discussions with them and with Dr. J. P. Schiffer.

APPENDIX: CLASSICAL MODEL OF ANGULAR-MOMENTUM MATCHING

Let each nonelastic channel α consist of two uniform spheres with mass, charge, and radius (m_1, q_1, r_1) and (m_2, q_2, r_2). When they are touching, their moment of inertia about the center of mass is

$$\mathcal{I}=\mathcal{I}_1+\mathcal{I}_2+\mu R^2, \tag{A1}$$

where

$$\mathcal{I}_1=\tfrac{2}{5}m_1r_1^2, \quad \text{and} \quad \mathcal{I}_2=\tfrac{2}{5}m_2r_2^2,$$
$$R=r_1+r_2, \qquad \mu=m_1m_2/(m_1+m_2).$$

In the c.m. system, the separation velocity v of the two spheres is given by

$$\tfrac{1}{2}\mu v^2\approx E+Q-q_1q_2/R, \tag{A2}$$

where $-Q$ is the threshold energy of channel α and E is the available (c.m.) energy of the incoming beam. Semiclassically, the maximum angular momentum that the channel α can carry away is

$$\hbar L_c'(\alpha)\approx\mathcal{I}v/R,$$

i.e., the classical angular momentum when the vector **R** is perpendicular to the vector **v**. Finally,

$$L_c'(\alpha)\approx(1/\hbar R)\mathcal{I}[(2/\mu)(E+Q-q_1q_2/R)]^{1/2}. \tag{A3}$$

Then the cutoff L_c for absorption into any nonelastic channel is

$$L_c'=\max L_c'(\alpha). \tag{A4}$$

PHYSICAL REVIEW C VOLUME 1, NUMBER 3 MARCH 1970

Polarization in *n-d* Scattering at 7.8 MeV*

J. TAYLOR,† G. SPALEK, TH. STAMMBACH, R. A. HARDEKOPF,‡ AND R. L. WALTER
Department of Physics, Duke University, Durham, North Carolina 27706 and
Triangle Universities Nuclear Laboratory, Durham, North Carolina 27706
(Received 16 October 1969)

Asymmetries produced in the scattering of 7.8-MeV polarized neutrons have been measured to an accuracy better than ±0.020 for 12 angles ranging from 58° to 165° (c.m.). The ^{9}Be(α, n_0) reaction was employed as a neutron source with a polarization of 0.539±0.012. The measured asymmetries agree with the 8-MeV data for the charge-symmetric *p-d* scattering, indicating that the Coulomb effects are indeed small at this energy. The data also follow the trend of the 9-MeV calculation of Purrington and Gammel.

I. INTRODUCTION

As the two-nucleon problem becomes better understood, more interest is being directed to the three-nucleon problem, both experimentally as well as theoretically. The complexity in describing the three-nucleon problem accurately is much larger because the experiments use the deuteron, a particle with spin 1 and with a ground state having around 4% *D*-state admixture. Thus, many parameters, e.g., phase shifts and mixing coefficients, are involved in the representation of nucleon-deuteron scattering. Also, if one is looking for possibly weak effects, such as the three-nucleon force or charge-dependent interactions, one needs a wealth of data from a variety of polarization experiments. Work along these lines is now proceeding for the *p-d* interaction. The most straightforward polarization experiment, the scattering of polarized protons from deuterons, has been performed recently at many energies above 4 MeV with the high accuracy attainable with a charged-particle polarized-ion source.[1–6] In contrast, no major experimental contribution to the neutron-deuteron polarization problem has been made for energies below 20 MeV since the survey reported six years ago by Walter and Kelsey who presented polarization angular distributions at five energies.[7]

Theoretical calculations of the polarization phe-

* Work supported by the U.S. Atomic Energy Commission.
† National Defense Education Act Fellow.
‡ Woodrow Wilson Fellow.

[1] W. Grüebler, W. Haeberli, and P. Extermann, Nucl. Phys. **77**, 394 (1966).
[2] T. B. Clegg and W. Haeberli, Nucl. Phys. **A95**, 608 (1967).
[3] J. H. P. C. Megaw, A. R. Johnston, W. R. Gibson, and F. G. Kingston, Nucl. Phys. **A122**, 689 (1968).
[4] J. C. Faivre, D. Garreta, J. Jungerman, A. Papineau, J. Sura, and A. Tarrats, Nucl. Phys. **A127**, 169 (1969).
[5] J. S. C. McKee, D. J. Clarke, R. J. Slobodrian, and W. F. Tivol, Phys. Letters **24B**, 240 (1967).
[6] J. S. C. McKee, A. U. Luccio, R. J. Slobodrian, and W. F. Tivol, Nucl. Phys. **A108**, 177 (1968).
[7] R. L. Walter and C. A. Kelsey, Nucl. Phys. **46**, 66 (1963).